Resistivity imaging and image analysis for estimating water and solute transport across the capillary fringe in laboratory experiments

TORLEIF DAHLIN[1], BENEDICT RUMPF[1], PONTUS POJMARK[2], KRISTOFER HELLMAN[1], MAGNUS PERSSON[2] and THOMAS GÜNTHER[3]

[1] Engineering Geology, Lund University, Box 118, 211 00 Lund, Sweden.
[2] Water Resources Engineering, Lund University, Box 118, 211 00 Lund, Sweden.
[3] Leibniz Institute for Applied Geophysics, Stilleweg 2, 30655 Hannover, Germany.

Torleif.Dahlin@tg.lth.se

Introduction

The rapid population growth combined with industrialisation and urbanisation results in an increasing demand for water and threatens the livelihoods of many people. Therefore, the maintenance and protection of groundwater, the largest freshwater resource in many areas, becomes one of the biggest challenges of our times. To assure a secure water supply for drinking, industry and agriculture it is essential to avoid groundwater contaminations and therefore to understand the subsurface water movement.

The hydrological cycle and its steps between precipitation and groundwater runoff are well known and were described e.g. by FETTER (2001), or PRESS and SIEVER (2003). The saturated as well as the unsaturated zone have been subject of many water movement surveys over the last decades (see e.g. WELLINGS and BELL, 1982; MCMAHON et al., 2001; MALI et al., 2006; MIKULEC and ORFANUS, 2005). However, the influence and complexity of the region of transition between these zones, the capillary fringe, has been more or less neglected in water movement investigations. Although a lateral movement of water within the capillary fringe was recognized already by LUTHIN and DAY (1955), the role of the capillary fringe in lateral transport of water and pollutants has not completely been explained in groundwater literature. Recent studies showed that this role might be more significant than expected.

The aim of this study was to analyse the lateral movement of water and solutes in the capillary fringe, regarding the impacts of the unsaturated infiltration rate and the hydraulic gradient of the groundwater table, by using a combination of image analysis and geoelectrical monitoring.

Method Description

The model used in this study involved a 150 cm long, 49 cm high and 48 cm deep glass aquarium. It consisted of 3 basins which were separated by perforated walls covered with a permeable geotextile. The main basin had a width of 122 cm and was situated between two smaller basins, each with a width of 10 cm. The main basin was filled up to a height of 32 cm with homogeneous sand. The sand had a grain size of 0.3-0.7 mm and allowed a capillary fringe of 13 cm above the saturated zone. The thickness of the saturated zone could be regulated by changing the water levels in the two smaller basins on both sides of the aquarium. A pump system was installed to circulate water through the aquarium and regulate the gradient across the basin. The maximum water level varied between 9 and 12 cm. Therefore it was possible to establish a three-layer regime within the aquarium, including the saturated zone, the capillary fringe and an unsaturated zone of approximately 8-10 cm on top.

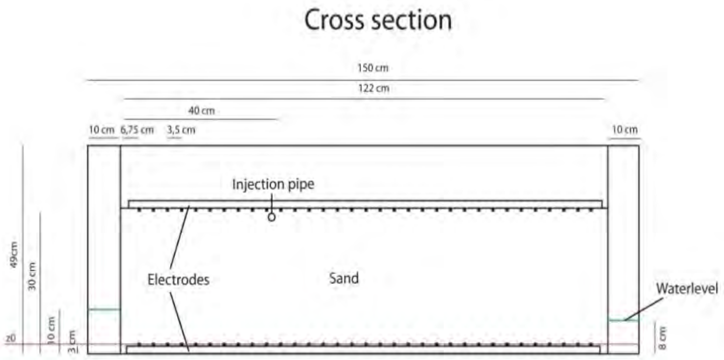

Fig. 1: Cross section of the aquarium layout.

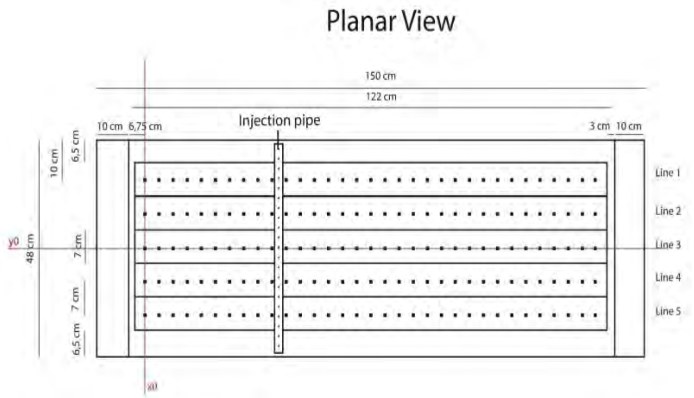

Fig. 2: Planar view of the aquarium layout.

Infiltration of the dye tracer Brilliant Blue FCF was regulated by a pump and injected through a pipe system on the sand surface. To keep the same water levels, even after the injection of the dye tracer, another pump was connected to a level gauge in the right basin, which extracted the same amount of water that was injected in form of the tracer. The cross sections of the aquarium can be seen in Figure 1 and 2, and a photograph of the laboratory setup is shown in Figure 3.

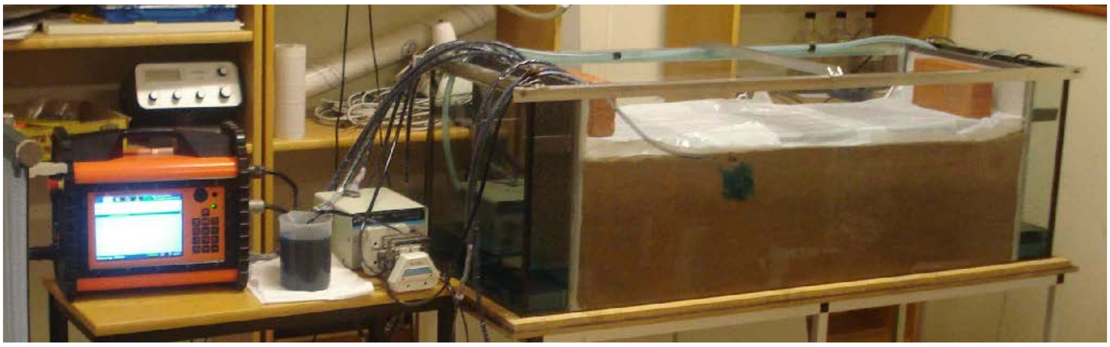

Fig. 3: Laboratory setup of the aquarium during tracer injection.

Photographs taken at a regular time interval of 3 minutes were used for the image analysis to visualize the flow paths through the front side of the aquarium. Every tenth picture, which corresponds to a time interval of 30 minutes, was modified with Adobe Photoshop CS ™ and Adobe Illustrator CS ™ to create a black and white template image. These modified template images were then combined to present the tracer distribution throughout the experiments in relation to the soil water regime within the aquarium.

An ABEM Terrameter LS was connected to a customised electrode system to measure the resistivity data during the experiments. Ten lines of electrodes were used; five in the bottom and five on top of the sand, containing a total of 320 electrodes (see Figure 1 and Figure 2). The electrode spacing was 3.5 cm. A combination of multiple-gradient array and cross-hole-dipole-dipole array was used for taking measurements along and between the electrodes on top of and in the bottom of the sand.

The Boundless Electrical Resistivity Tomography (BERT) software, which is described in GÜNTHER et al. (2006), was used to obtain a three dimensional model of the resistivity distribution within the aquarium. The dimensions and boundary conditions of the aquarium were incorporated in the model and different inversion parameters were adjusted to improve the model quality. A MATLAB ® script created a ratio between the resistivity values taken during the experiments and a background measurement which was taken before each experiment. ParaView was used to visualise the gained model with a 'blue to white' colour scheme. Blue colour represents ratio values smaller than 1, which corresponds to a decrease of resistivity. Areas with no change in resistivity (ratio = 1) were presented white.

The results of the geoelectrical monitoring were evaluated in respect to the correlation of the results of the image analysis by comparing the side views of the 3D ratio plots with the corresponding shape of the dye distribution from the image analysis.

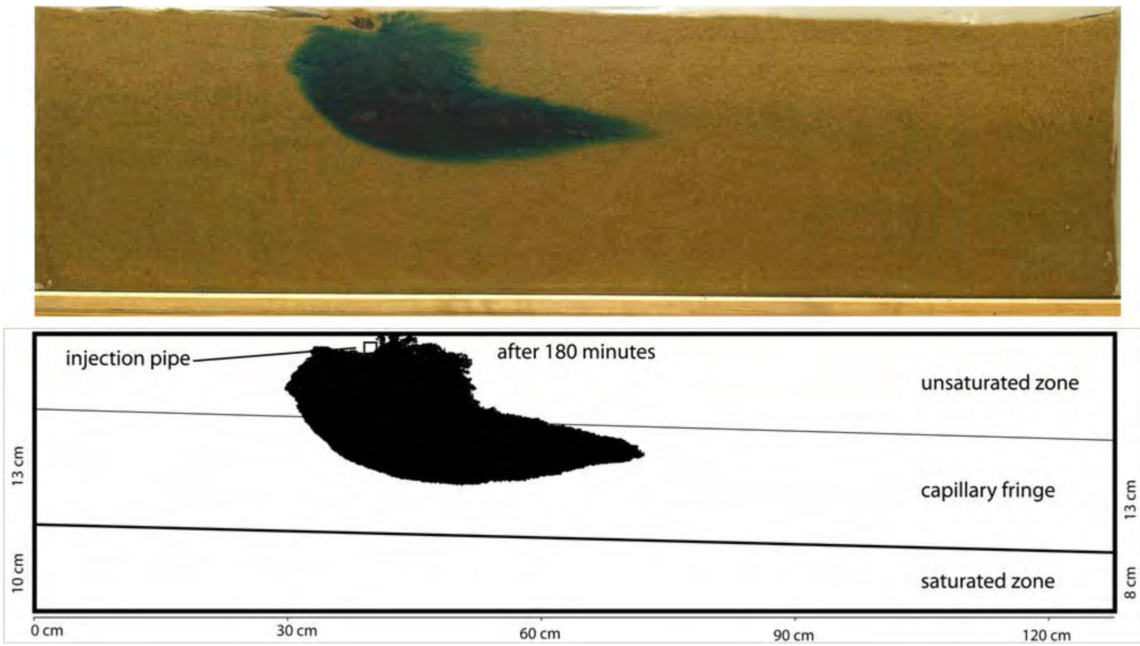

Fig. 4: Image analysis result from experiment 1 after 180 minutes, shown as photograph (upper) and outline of tracer plume from image analysis (lower).

Results and Discussion

Five experiments were conducted to investigate the lateral movement of the dye tracer within the capillary fringe of sand. All experiments revealed a strong horizontal movement across the capillary fringe, but only experiment 1 is presented here. The results of the image analysis (Fig. 4) show that the infiltrated dye tracer percolated vertically through the unsaturated zone, but moved horizontally as soon as it reached the capillary fringe, without intersecting the saturated zone.

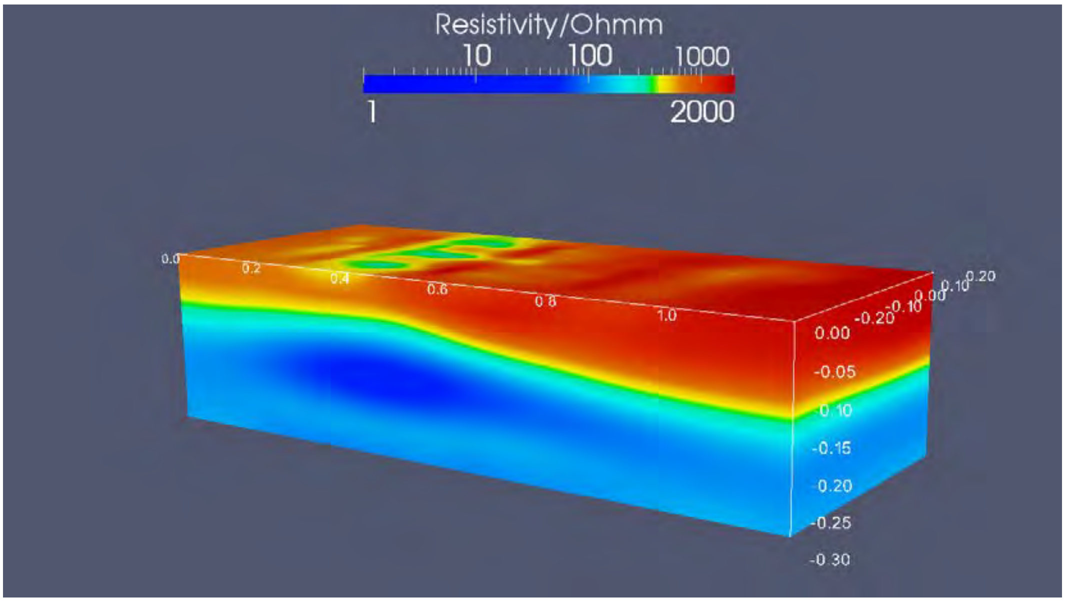

Fig. 5: 3D resistivity model from experiment 1 after 180 minutes.

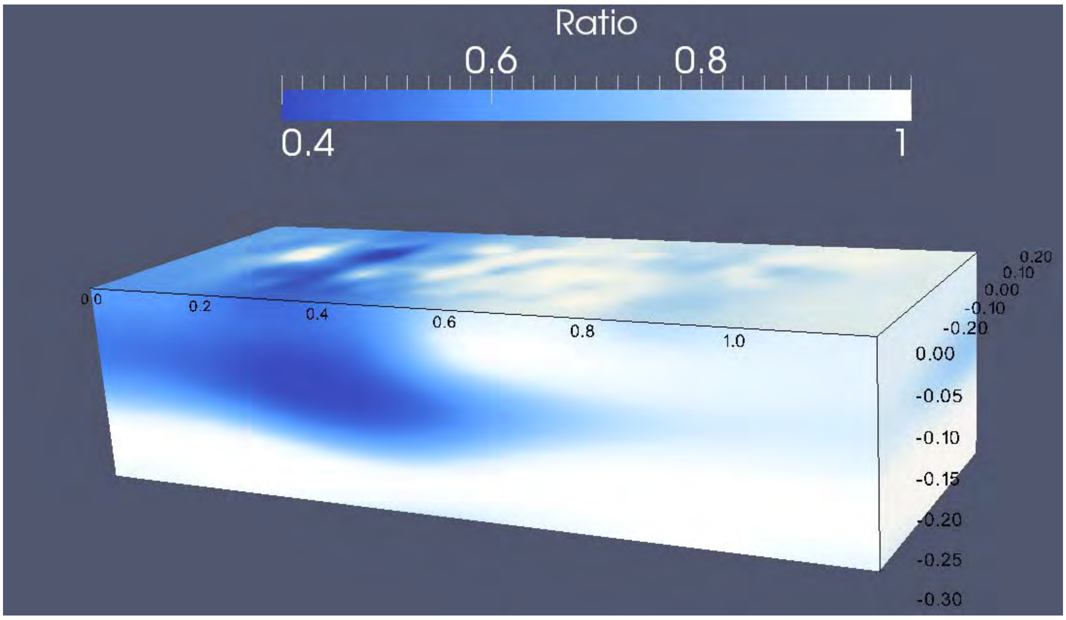

Fig. 6: 3D model of change in resistivity relative to before injection started from experiment 1 after 180 minutes.

The corresponding resistivity model resulting from inversion with BERT is shown in Fig. 5. Although the position and centre of the low resistive anomaly is easy to see, the result is clearer and easier to interpret by presenting a model of the change in resistivity since before tracer injection started as shown in Fig. 6. An overall similarity of the shapes of the dye distributions can be seen in all experiments. In general, the plumes of the resistivity difference models are bigger than the plumes of the image analyses and seem to have smoother borders. However it must be considered that the borders of the image analysis only seem to be that sharp because of the schematic presentation method. The original photographs show a decreasing concentration of dye in the outer parts of the plume. The difference in the sizes of the plumes can be explained with the different minimal detection limits of the methods. While the resistivity analysis can measure even smallest changes caused by minimal variations in the concentration of dye, the lowest with human eyes detectable concentration of dye in sand is about 0.1 g/l.

It is interesting to note that in all experiments even if the plume of the modelled dye tracer distribution is bigger than the one seen in the image analysis, the dye never reaches the saturated zone.

Conclusions

The goal of this study was to analyse the water and solute transport across the capillary fringe using a combination of image and resistivity analysis. The comparison between the image analysis and the side views of the 3D models showed a clear correlation and therefore indicate a high reliability for the inversion. The models gave a clear impression of the dye distribution in the whole aquarium and proved that resistivity monitoring is a very useful tool for tracing subsurface processes involving change in water saturation or chemical composition.

The comparison of the experiments with different hydraulic gradients and infiltration rates revealed a high horizontal movement across the capillary fringe. In all experiments, the dye tracer moved vertically through the unsaturated zone, but moved laterally within the capillary fringe without intersecting the saturated zone.

The flow characteristics of the capillary fringe turned out to be more similar to the characteristics of the saturated zone, than to the characteristics of the unsaturated zone. If the result of this laboratory study can be verified under field conditions, it clearly shows that taking measurements and samples only in the saturated zone at contaminated sites can significantly underestimate the actual extent of the contamination plume.

Acknowledgements

The work presented here was funded by a research grant from Swedish Geological Survey.

References

FETTER, C.W., 2001: Applied Hydrogeology. – Fourth Edition, 598 S., Prentice-Hall Inc.

GÜNTHER, T., RÜCKER, C. and SPITZER, K., 2006: 3-D modelling and inversion of dc resistivity data incorporating topography – part II: Inversion. – Geophysical Journal International, **166**(2), 506-517.

LUTHIN, J.N. and DAY, P.R., 1955: Lateral flow above a sloping water table. – Proceedings of the Soil Science Society of America, **19**, 406 - 410.

MALI, N., URBANC, J. and LEIS, A., 2006: Tracing of water movement through the unsaturated zone of a coarse gravel aquifer by means of dye and deuterated water. – Environmental Geology, **51**(8), 1401-1412.

McMahon, P.B., Dennehy, K.F., Michel, R.L., Sophocleous, M.A., Ellet, K.M. and Hurlbut, D.B., 2001: Water Movement Through Thick Unsaturated Zones Overlying the Central High Plains Aquifer, Southwestern Kansas, 2000-2001. – USGS, Water Resources Investigations Report 03-4171, 32.

Mikulec, V. and Orfanus, T., 2005: Numerical Simulation of Soil Water Movement in Variably Saturated Zone of Heterogeneous Soil Profile during Growing Period of Corn. – Geophysical Research Abstracts, **7**, European Geoscience Union.

Press, F. and Siever, R., 2003: Allgemeine Geologie, Einführung in das System Erde, 3. Auflage, Spektrum.

Wellings, S.R. and Bell, J.P., 1982: Physical controls of water movement in the unsaturated zone. – Quarterly Journal of Engineering Geology and Hydrogeology, **15**, 235-241.